

DETERMINATION OF SOIL-STRUCTURE INTERACTION EFFECTS FOR A MODEL TEST STRUCTURE USING PARAMETRIC SYSTEM IDENTIFICATION PROCEDURES

Salih Tileylioglu¹, Robert L. Nigbor², and Jonathan P. Stewart³

¹ PhD. Candidate, Department of Civil and Environmental Engineering, Boelter Hall 6689, University of California, Los Angeles, CA 90095; email: saliht@ucla.edu

² Researcher, Department of Civil and Environmental Engineering, Boelter Hall 6689, University of California, Los Angeles, CA 90095; email: nigbor@ucla.edu

³ Professor and Vice Chair, Department of Civil and Environmental Engineering, Boelter Hall 6689, University of California, Los Angeles, CA 90095; email: jstewart@seas.ucla.edu

ABSTRACT: Earthquake recordings from a model test structure located at Garner Valley California are used to evaluate inertial soil-structure interaction (SSI) effects. The test structure consists of steel columns and bracings 4.06 m in height supporting a $4m \times 4m \times 0.4m$ reinforced concrete roof slab. The structure rests on a $4m \times 4m \times 0.5m$ reinforced concrete foundation with no embedment. Surficial soil conditions consist of organic soil overlying silty sand alluvium with an average shear wave velocity in the upper 15 m of 200m/s. Seismic monitoring is performed with uni-axial (horizontal) accelerometers on the roof and foundation as well as vertical sensors at the corners of the foundation. Parametric system identification procedures are implemented to evaluate fundamental-mode vibration frequencies for a fixed- and flexible-base condition, from which SSI effects can be inferred. Data is available for the structure with and without bracing from two earthquakes. The lengthening of the fixed-base period due to SSI is a period lengthening of 12% and 74% for the braced and unbraced structure, respectively. The corresponding foundation damping levels for these two cases are about 1% and 5%. The different levels of period lengthening and foundation damping for the two structural configurations reflect the strong increase of inertial SSI effects with the ratio of structure-to-soil stiffness, which is naturally greater for the fixed- base configuration. The observed levels of SSI are reasonably well predicted by available theoretical models.

INTRODUCTION

Both inertial and kinematic soil-structure interaction (SSI) effects can contribute to the response of a structure resting on a compliant geologic medium. Kinematic interaction principally affects the frequency content and amplitude of foundation motions relative to free-field motions (e.g., Veletsos and Prasad, 1989). Inertial interaction is fundamentally related to the foundation rotations and displacements, as well as the energy dissipation, that occurs when base shear and moment is applied to the foundations by the vibrating structure. In some conditions, those foundation

rotations and displacements can represent a significant fraction of the total soil-foundation-structure system flexibility. Similarly, the radiation and hysteretic damping associated with the foundation acting as a wave source into the surrounding geologic medium can significantly contribute to the overall system damping. These inertial interaction effects can be concisely expressed by their impact on modal vibration frequencies and damping ratios. These parameters are termed as “flexible-base” for a structure on a compliant base and “fixed- based” for the fictional case of a structure resting on a rigid base.

Theoretical models have existed for many years to predict inertial SSI effects on the period and damping ratio of a single degree of freedom oscillator (e.g., Bielak, 1975; Veletsos and Nair, 1975). Previous studies have sought to validate those studies using strong motion data from instrumented structures (e.g., Stewart et al., 1999a, b) and forced-vibration data (e.g., Luco and de Barros, 2004). We extend that work by investigating SSI effects on the fundamental-mode period and damping ratio of a well instrumented model test structure. This extends previous work in several respects: (1) the resolution of the sensors and quality of the data acquisition system allows more accurate evaluation of SSI effects than has been possible previously; (2) the test structure is reconfigurable so that SSI effects for different levels of structural stiffness, but constant foundation and soil conditions, can be evaluated; (3) SSI effects can be evaluated for three vibration sources including ambient, a mounted shaker, and earthquakes.

The test structure was constructed in 2004 and is located in Garner Valley, California. It is owned and operated by the NEES site at UCSB (Nigbor et al., 2004; Steidl et al., 2004; <http://nees.ucsb.edu>).

The paper begins with a general overview of the site and structure. The system identification procedures used to evaluate modal parameters for different base fixity conditions are then presented along with the results. Those results are then interpreted to evaluate SSI effects, which are compared to predictions of a theoretical model.

SITE AND STRUCTURE DESCRIPTION

The test structure is located in a sedimentary basin that is instrumented as part of the Garner Valley Differential Array (GVDA). Garner Valley, California is in a region of high seismicity. As shown in Figure 1, soil conditions consist of organics at the top and silty sand extending to a depth of 18 *m*, which then transitions to decomposed granite. Relatively intact crystalline bedrock occurs at a depth of 88 *m*. The ground water table is at the surface in rainy seasons and drops to about 3 *m* in dry seasons. Geophysical tests (suspension logging and SASW) have been carried out to measure P- and S-wave velocity profiles. The SASW analysis indicates near-surface shear wave velocity, $V_s = 207$ *m/s*.

The test structure was constructed specifically to facilitate SSI experiments and hence is referred to as the soil-foundation-structure interaction (SFSI) test structure. As shown in Figure 2, the structure consists of a simple steel frame supporting a roof slab 40 cm in thickness. The foundation consists of a non-embedded reinforced concrete slab 50 cm thick. The height of the structure from base of foundation to top of roof slab is 4.56 m. The plan dimensions of the foundation and roof slabs are 4m x

4m. Reconfigurable bracings can be inserted within the structure to modify its vibration characteristics.

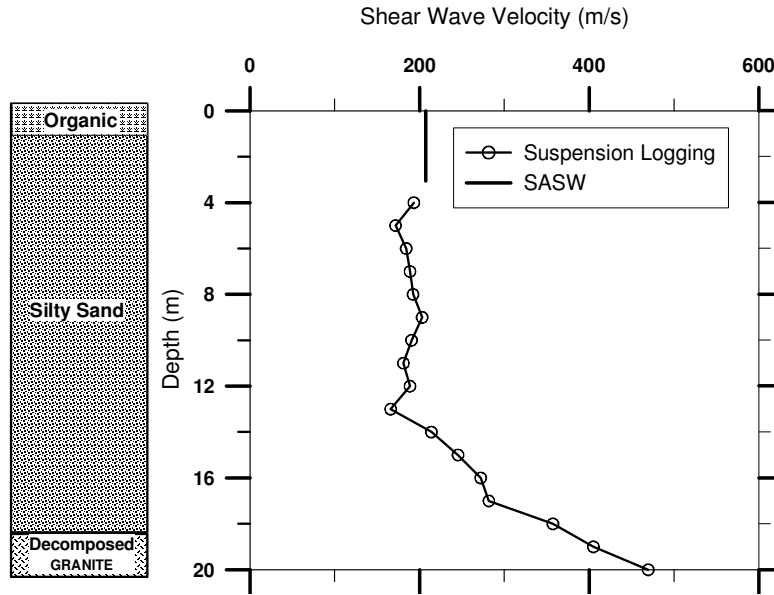


FIG. 1. Near surface soil profile with shear wave velocities obtained from suspension logging and SASW tests

The SFSI test structure is instrumented with triaxial and uniaxial accelerometers and pressure sensors. The structure is located within the broader GVDA, which consists of free-field triaxial accelerometers positioned across Garner Valley. A downhole array is also present near the structure. Sensor signals are digitally recorded with a resolution of 24-bits and a sample rate of 200 samples per second. Several earthquakes have been recorded with magnitudes of 5 or less. In this paper we consider two earthquakes with $M_L=3.5$ and $M_w=4.9$.

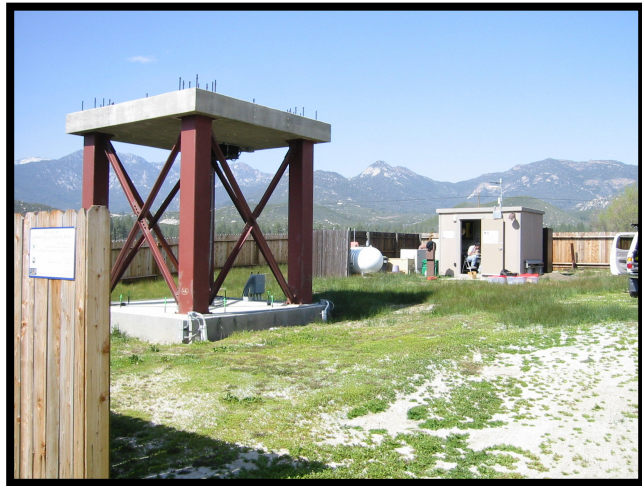


FIG. 2. The SFSI test structure at GVDA with bracings in place

Unfortunately, free-field data are not available for these events. Base-of-structure peak accelerations for these two events were 0.008g and 0.05g, respectively. The $M_L = 3.5$ event is used for system identification without bracing and the $M_L = 4.9$ event is used for system identification with bracing.

SYSTEM IDENTIFICATION

Ground motion recordings and forced vibration tests may be used in system identification procedures to estimate modal vibration parameters of the soil-structure system. System identification is a process by which the properties of an unknown system are estimated based on a measured input to the system and output from the system. When different input-output pairs are utilized, the system itself changes. Referring to Figure 3, the base-of-structure recording can be visualized as being the sum of the free-field ground motion (u_g) and the relative free-field/foundation motion (u_f). This motion is modified at the roof of the structure as a result of base rotation (θH) and deformations of the structure itself (u). Hence, if u_g is taken as input and roof motion is taken as output, the intervening system has contributions from base translation, base rotation, and structure deformation, and is referred to as the flexible-base condition. Similarly, if the sum of base translation and θH is taken as input and roof translation as output, the intervening system is the structure alone, and the identified properties are referred to as fixed-base. The pseudo flexible-base case is an intervening case that neglects base translation, as indicated in Figure 3. Formal derivations of the above input-output pairs are given in Stewart and Fenves (1998).

A general measure of SSI effects can be obtained by comparing fixed-base and flexible-base parameters. One of the important effects of soil-structure interaction is to increase the system period with respect to the fixed-base case. This phenomenon is called period lengthening. Another important effect of SSI is to introduce foundation damping, which includes contributions from radiation damping and hysteretic material damping. This is expressed by a foundation damping factor (β_f) that is expressed as follows (Bielak, 1975; Veletsos and Nair, 1975):

where $\tilde{\beta}$ =flexible-base damping, β =fixed-base damping, \tilde{T} =flexible-base period, and T =fixed-base period.

We use a parametric system identification procedures described in detail by Stewart and Fenves (1998) to evaluate fundamental-mode frequencies and damping ratios. In this procedure, the system is assumed to consist of a multi degree-of-freedom structure

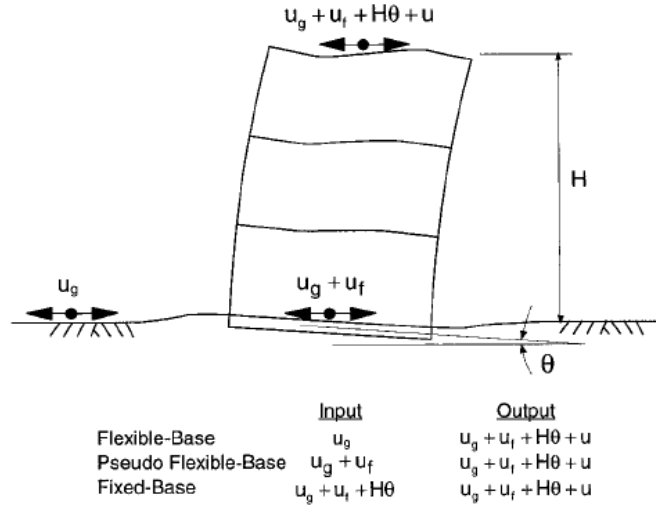


FIG. 3. Inputs and Outputs for System Identification analysis of a building (after Stewart et al., 1999)

with lumped masses. The procedure maps inputs to outputs via a transfer function surface defined in the Laplace domain (parametric procedure). The surface is defined as a function of both frequency and damping. The ordinates of the surface are evaluated so as to minimize the cumulative error between the model output and the recorded output. The peaks in the surface define modal frequencies and damping ratios.

Parametric system identification requires two user-specified parameters; the time delay between the input and output signals and the number of modes required to capture the response of the system. This is illustrated in Figure 4 for a particular input-output pair (structure without bracing, pseudo-flexible- base input-output pair). The minimum error occurs at a time delay of 2. The error for the number of modes essentially does not change significantly for number of modes > 4 .

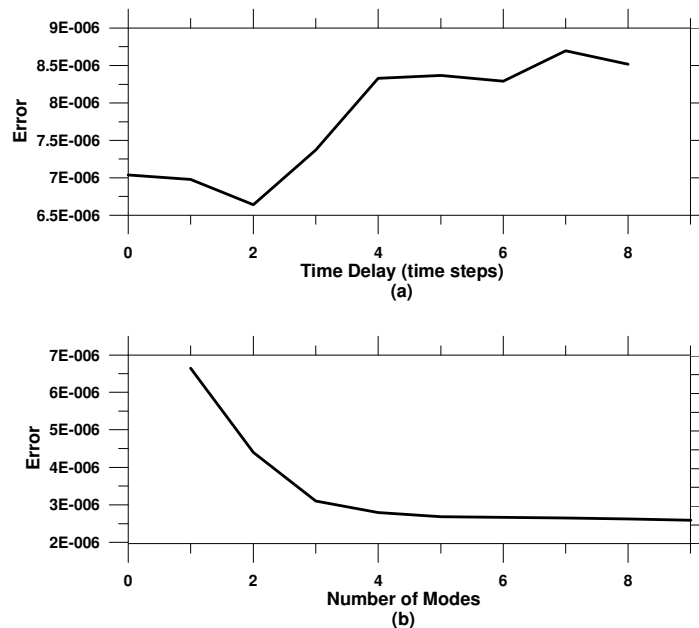


FIG.4. Error of system identification model with respect to (a) Time delay and (b) Number of modes

Using the aforementioned time lag and number of modes, the transfer function surface is identified as shown in Figure 5. Locations of high points (“poles”) and low points (“zeros”) are obtained that define the modal frequencies and damping ratios. Figure 6 compares a slice through the parametric transfer functions on the frequency axis and its comparison to a transmissibility function defined from smoothed power spectral density functions of the input and output (Pandit, 1991; Stewart and Fenves, 1998). We note that the frequencies of the major peaks match reasonably well. The amplitudes need not match as the transmissibility function depends on the smoothing procedure utilized (Stewart et al. 1999). As shown in Figure 7, another check consists of comparing the time series output of the parametric model to data, which indicates a reasonable match.

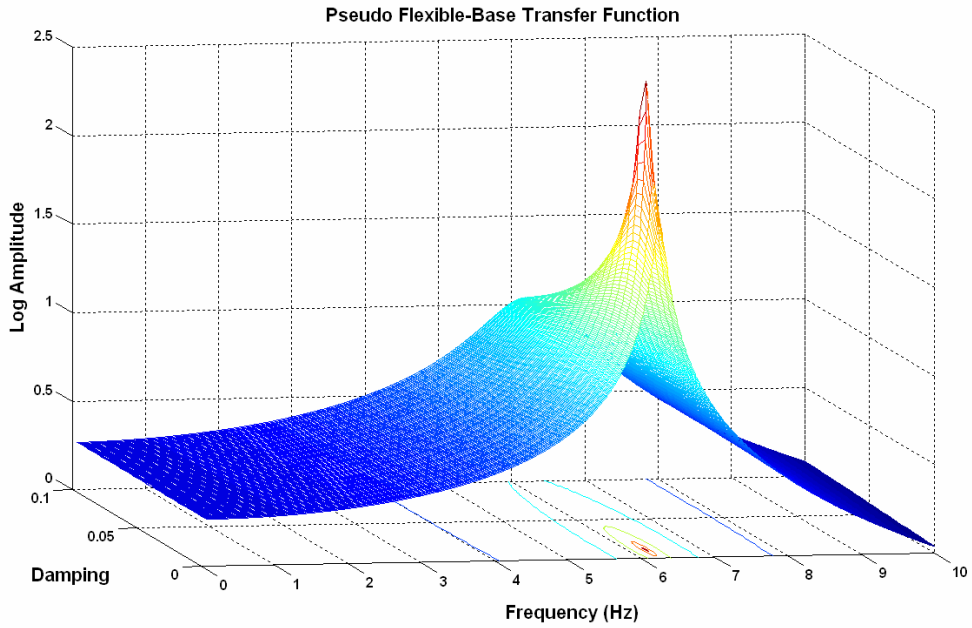


FIG.5. Transfer function surface (pseudo flexible-base case, no bracing)

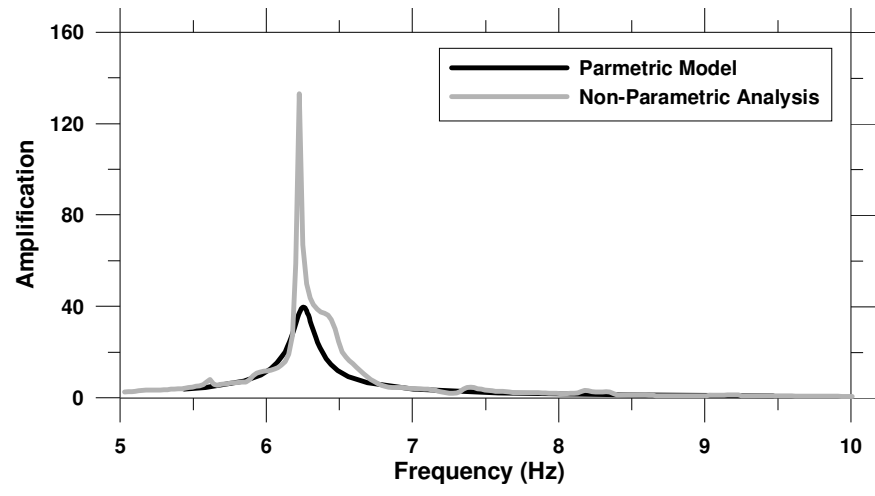


FIG.6. Comparison of transfer function from parametric system identification and transmissibility function obtained from smoothed power spectral densities of input and output signals (pseudo flexible-base case, no bracing)

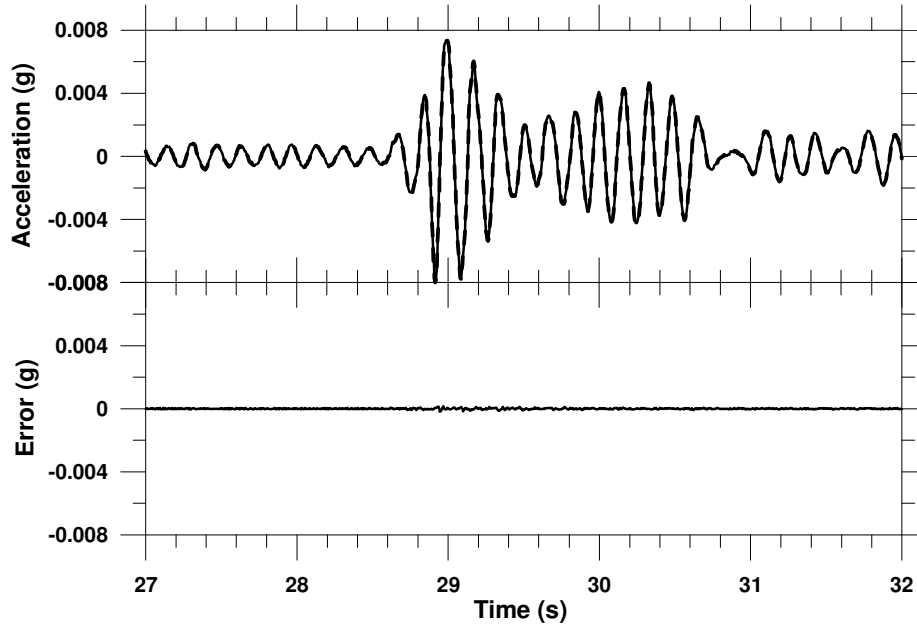


FIG.7. The output recording compared to the model output and the difference between the two motions (bottom)

The result of this analysis is that pseudo flexible-base first-mode frequency and damping ratio are estimated as 6.25 Hz and 1.1%. Repeating these analyses for the fixed-base input-output pair and for the braced structure yields the results given in Table 1. The reduction in frequency and increase of damping of pseudo flexible-base parameters relative to fixed-base parameters indicates an inertial SSI effect for this structure.

Table 1. Summary of system identification from ground motions

Structural Configuration	Peak motion at top of structure (g)	Fixed-Base Parameters		Pseudo Flexible- Base Parameters	
		f (Hz)	β (%)	f (Hz)	β (%)
Unbraced	0.008	7.0±0.001	0.20±0.003	6.25±0.001	1.10±0.004
Braced	0.05	16.20±0.005	3.0±0.01	9.70±0.001	5.60±0

INTERPRETATION

The lack of free-field data prevented the calculation of flexible- base parameters from system identification. However, those parameters may be estimated using a procedure described by Stewart and Fenves (1998). For the case of known fixed- and pseudo flexible-base parameters, the flexible-base frequency is calculated as follows:

$$\tilde{\omega}^2 = \frac{1}{1/\omega^2 + 1/\omega_\theta^2 + 1/\omega_u^2} \quad (2)$$

Parameter ω =fixed-base circular frequency, ω_u =vibration frequency related to foundation translation, and ω_θ =vibration frequency related to foundation rotation, which is estimated as:

$$\frac{1}{\omega_\theta^2} = \frac{1}{(\omega^*)^2} - \frac{1}{\omega^2} \quad (3)$$

where ω^* =pseudo flexible-base circular frequency. Parameter ω_u is calculated from:

$$\left(\frac{\omega_\theta}{\omega_u}\right)^2 = \left(\frac{r_\theta^3}{r_u h^2}\right) \left(\frac{2-v}{3(1-v)}\right) \left(\frac{\alpha_\theta}{\alpha_u}\right) \quad (4)$$

Parameters r_θ and r_u are the equivalent radii which match the moment of inertia and area of the foundation, respectively, v =Poisson's ratio of soil, h =height of structure, and α_θ and α_u represent frequency-dependent dynamic modifier factors to the static foundation rotational and translational stiffness, respectively (e.g., Veletsos and Verbic, 1973).

Similarly, the flexible-base damping ratio ($\tilde{\beta}$) is calculated from:

$$\tilde{\beta} = \left(\frac{\tilde{\omega}}{\omega_u}\right)^3 \beta_u + \left(\frac{\tilde{\omega}}{\omega}\right)^3 \beta + \left(\frac{\tilde{\omega}}{\omega_\theta}\right)^3 \beta_\theta \quad (5)$$

where β_θ and β_u are given by:

$$\beta_\theta = \frac{\tilde{\beta}^* - \beta(\tilde{\omega}^*/\omega)^3}{(\omega^*/\omega_\theta)^3} \quad (6)$$

$$\beta_u = \beta_\theta \frac{\omega_\theta c_u h^2 r_u^2}{\omega_u c_\theta r_\theta^4} \frac{3(1-v)}{2-v} \quad (7)$$

in which $\tilde{\beta}^*$ is the pseudo flexible-base damping, β =fixed-base damping, and β_u and β_θ are frequency dependent dynamic factors used for the calculation of the complex-part of foundation impedance functions (e.g., Veletsos and Verbic, 1973).

Table 2 summarizes the flexible-base frequency \tilde{f} and damping ratio $\tilde{\beta}$ estimated using the above process. The flexible-base parameters are similar to the pseudo flexible-base parameters, because foundation rocking is the dominant SSI effect in this case.

Table 2. Estimated flexible-base parameters, SSI effects inferred from data, and SSI effects predicted by model

Structural Configuration	Flexible-Base Parameters		SSI Effect: Data		SSI Effect: Model	
	\tilde{f} (Hz)	$\tilde{\beta}$ (%)	\tilde{T}/T	β_f (%)	\tilde{T}/T	β_f (%)
Unbraced	6.13	1.11	1.14	0.96	1.10	1.40
Braced	9.20	4.80	1.76	4.20	1.55	5.30

As shown in Table 2, period lengthening and foundation damping (per Eq. 1) are calculated from the fixed-base parameters in Table 1 and the estimated flexible-base parameters in Table 2. The period lengthening and foundation are much larger for the braced configuration because of the stiffer structural system. Those results are compared to theoretical predictions for a rigid circular foundation on viscoelastic halfspace. The theoretical formulation, which is modified from Veletsos and Nair (1975), is described by Kramer and Stewart (2004). The model underpredicts the observed period lengthening and foundation damping in both cases, although the residuals are modest and the model captures well the differences between the unbraced and brace cases.

CONCLUSIONS

In this article, we have described the SFSI test structure in Garner Valley, which is an excellent experimental facility for detailed examination of SSI effects. Parametric system identification procedures were performed to examine the effects of SSI on the fundamental mode period and damping ratio. Results are obtained with the structure in a braced and unbraced configuration, which provides significantly different levels of SSI effects. The foundation damping and period lengthening calculated were found to be 0.96% and 1.14, respectively for the unbraced configuration. The values were 4.2% and 1.76 for the braced configuration. The results obtained from the system identification apply for small-strain conditions due to the weak shaking during the subject earthquakes. Strong ground motions have not yet been recorded by this array.

ACKNOWLEDGMENTS

The authors thank support from CENS. Special thanks to Ali Asghari for his help in the reconfigurations of the bracings in the structure.

REFERENCES

- Bielak, J. (1975). "Dynamic behavior of structures with embedded foundations." *J. Earthquake Engrg. Struct. Dyn.*, 3 (3), 259–274.
- Kramer, S.L. and Stewart, J.P. (2004). Chapter 4: "Geotechnical Aspects of Seismic Hazards," in *Earthquake Engineering. From Engineering Seismology to Performance-Based Engineering*, Y. Bozorgnia and V.V. Bertero (editors), CRC Press, 85 pages.
- Luco, J. E and de Barros, F.C.P (2004). "Assessment of predictions of the response of the Hualien containment model during forced vibration tests," *J. Earthquake Engrg. Struct. Dyn.*, 24 (12), 1013–1035.
- Nigbor, R., Asghari, A., McMichael, L., and Mish, K., (2004). "Development of prototype SFSI simulation tool," *13WCEE*, Vancouver BC.
- Pandit, S. M. (1991). *Modal and spectrum analysis*. Wiley, New York.
- Steidl, J., Youd, T.L., and Nigbor, R.L. (2004)/ "Research Opportunities at the NEES permanently instrumented field sites," *13WCEE*, Vancouver BC.

- Stewart, J.P. and Fenves, G.L. (1998). "System identification for evaluating soil-structure interaction effects in buildings from strong motion recordings," *J. Earthquake Engrg. Struct. Dyn.*, 27 (8), 869-885.
- Stewart, J.P., Fenves, G.L. and Seed, R.B. (1999a). "Seismic soil-structure interaction in buildings. I: Analytical aspects," *J. Geotech. & Geoenv. Engrg.*, ASCE, 125 (1), 26-37.
- Stewart, J.P., Seed, R.B., and Fenves, G.L. (1999b). "Seismic soil-structure interaction in buildings. II: Empirical findings," *J. Geotech. & Geoenv. Engrg.*, ASCE, 125 (1), 38-48.
- Veletsos, A. S., and Nair, V. V. (1975). "Seismic interaction of structures on hysteretic foundations." *J. Struct. Engrg.*, ASCE, 101(1), 109-129.
- Veletsos, A.S and Prasad, (1989). "Seismic interaction of structures and soils: stochastic approach," *J. Struct. Engrg.*, ASCE, 115(4), 935-956,
- Veletsos, A. S., and Verbic, B. (1973). "Vibration of viscoelastic foundations." *J. Earthquake Engrg. Struct. Dyn.*, 2 (1), 87-102.